Available online at www.sciencedirect.com
ScienceDirect
International Journal of Heat and Mass Transfer 50 (2007) 2537–2544
International Journal of HEAT and MASS TRANSFER
www.elsevier.com/locate/ijhmt

# A thermal-ablation bioheat model including liquid-to-vapor phase change, pressure- and necrosis-dependent perfusion, and moisture-dependent properties

J.P. Abraham [a,*], E.M. Sparrow [b]

[a] Laboratory for Heat Transfer Practice, School of Engineering, University of St. Thomas, St. Paul, MN 55105-1079, United States
[b] Laboratory for Heat Transfer Practice, Department of Mechanical Engineering, University of Minnesota, Minneapolis, MN 55455-0111, United States

Received 29 September 2006; received in revised form 29 November 2006
Available online 9 March 2007

**Abstract**

A new bioheat model is applied to evaluate the use of elevated-temperature thermal therapies for the non-surgical ablation of diseased tissue. The new model is based on the use of the enthalpy method to account for liquid-to-vapor phase change. In addition, the model includes thermophysical property dependence on liquid content and variations of blood perfusion rates dependent on the local necrotic state of the tissue or external pressure applied by the therapy-delivering device. This model is applied here specifically to endometrial ablation for the treatment of menorrhagia. The results of the implementation of the model yielded the depth of tissue necrosis corresponding to a given application of heat at the exposed inner surface of the uterine tissue. These results definitively establish the occurrence of phase change and the complete suppression of perfusion as the major factors governing the necrosis depth. The accounting of moisture-dependent properties had a negligible effect on necrosis.


*Keywords:* Bioheat transfer; Endometrial ablation; Phase change; Blood perfusion variations; Enthalpy method; Tissue necrosis

## 1. Introduction

This paper is concerned with the development and implementation of a model to predict tissue necrosis during thermal-ablation therapy. Thermal therapy is used to treat various afflictions such as menorrhagia [1–3], cancer [4,5] and benign prostate hyperplasia [6–10]. Typical means of delivering thermotherapies include laser thermotherapy [11], application of heated liquids [1,3], microwave heating [5–7], among others.

The specific application of the model developed here is elevated-temperature-induced endometrial ablation which is used as a treatment of menorrhagia. The general approach to the implementation of thermal-ablation therapy is the controlled application of heat to the tissue bed. An elevated temperature front migrates through the tissue causing coagulative necrosis to the targeted tissue. Over time, the necrosed tissue is sloughed off, thereby completing the needed surgery.

The prediction of the depth to which necrosis will extend is a major issue with respect to the practical implementation of this therapy. In particular, the control of the depth of necrosis requires knowledge of the various parameters that govern the heat transfer process. The specific foci of the present investigation are threefold: (a) accounting of liquid-to-vapor phase change in the inter-tissue spaces, (b) consideration of the effect of water content on key thermophysical properties, and (c) taking account of the variation of perfusion with respect to both the necrotic state of the tissue and the pressure imposed by the therapeutic delivery system.

A painstaking review of the literature suggests that Baldwin et al. [1,3] were the first and, seemingly, the only group to investigate the role of inter-tissue liquid-to-vapor

* Corresponding author. Tel.: +1 651 962 5766; fax: +1 651 962 6419.
*E-mail address:* jpabraham@stthomas.edu (J.P. Abraham).

0017-9310/$ - see front matter © 2007 Elsevier Ltd. All rights reserved.
doi:10.1016/j.ijheatmasstransfer.2006.11.045

**Nomenclature**

| | |
|---|---|
| $c$ | specific heat (J/kg °C) |
| $C_{liq}$ | concentration of liquid |
| $h_{fg}$ | volumetric enthalpy of vaporization (J/m$^3$) |
| $h$ | volumetric enthalpy (J/m$^3$) |
| $k_t$ | thermal conductivity of tissue (W/m °C) |
| $Q_{met}$ | metabolic energy generation rate (W/m$^3$) |
| $R$ | universal gas constant (J/kmole K) |
| $t$ | time (s) |
| $T$ | temperature (°C) |
| $T_{core}$ | body core temperature (°C) |
| $x$ | coordinate location (m) |

*Greek symbols*

| | |
|---|---|
| $\Delta E$ | burn activation energy (J/mole) |
| $\delta$ | distance of phase front from uterine lining (m) |
| $\lambda$ | variable of integration |
| $\rho$ | density (kg/m$^3$) |
| $\xi$ | frequency factor (1/s) |
| $\omega$ | blood perfusion rate (1/s) |
| $\omega_0$ | initial blood perfusion rate (1/s) |
| $\Omega$ | tissue injury integral |

*Subscripts*

| | |
|---|---|
| b | blood |
| t | tissue |

*Superscripts*

| | |
|---|---|
| pre | zones which have not undergone phase change |
| post | zones which have undergone phase change |

phase change on the outcomes of thermal therapy processes. Consideration of their phase-change model suggests a potentially significant misapplication, the details of which will be elaborated later.

The present phase-change model is based on the *enthalpy method* [12], which has been successfully used in non-biomedical contexts [13–18]. The strength of the enthalpy method is that it naturally incorporates the latent heat of evaporation in the energy conservation equation which applies throughout the entire solution domain, thereby obviating the need to specifically track the location and velocity of the moving phase front.

The literature review also revealed the present status of the parameterization of blood perfusion, with special reference to the changes in perfusion that accompany necrosis. This knowledge is needed as background for incorporation into the present model. In this regard, a strong point of Baldwin's work is the attention given to the details of blood perfusion. Specifically, consideration was given to the response of perfusion to temperature, pressure, and thermal injury. These three factors were evaluated using the best available information at the time. The necessary information is a work-in-progress.

In the present model, a somewhat different approach to the effect of perfusion on energy transfer has been employed. First, very recent information on necrosis-affected blood perfusion has been taken into account [5]. Second, to provide an indication of the maximum effect of perfusion, the limiting case in which perfusion is totally suppressed was considered. In the present context, the suppression can be related to the pressure applied externally by the device which delivers the therapy.

The thermophysical properties which are relevant to a realistic model of the heat transport and necrosis processes are the thermal conductivity, the density, and the specific heat of the tissue. A key issue here is an understanding of what is meant by *tissue*. The writers view tissue as a composite of liquids, solids, and possibly water vapor. The water vapor component is a critical one which has, in the past, received virtually no consideration. If a given *volume* of tissue is considered, the constituents that compose that volume may change markedly during a heating period when there is a change of phase from liquid to vapor.

The values of the relevant thermophysical properties depend on temperature, composition, and necrotic state. It appears that greater attention has been given in the literature to the variation of the tissue properties with temperature than to the variations with composition. Major contributions to the temperature dependence of the properties have been reported [19–21]. Although there is a significant amount of information on the effect of temperature on the properties, it does not appear that this knowledge has been incorporated into any of the existing modeling efforts.

The effect of necrosis on property values has evoked only a minimum of investigation [5,22]. The information available from these investigations is insufficient to serve as a definitive input to a numerical simulation. Up to the present, the impact of necrosis on the properties has not been accounted for in modeling.

A number of experiments have been performed to determine the effect of liquid content on the relevant properties [20,21,23–27]. Based on the published data, the effect of composition on the values of the thermophysical properties appears to be of greater significance than the effect of temperature variations. Despite the presence of information about the thermophysical property dependence on composition, it does not appear that any of the current heat transport models have properly accounted for the variation of the properties with the instantaneous constituents of the tissue [1,3,28].

## 2. Model

### 2.1. The bioheat model

The starting point of the analysis is the Pennes bioheat equation [29], which is generalized here to take account of liquid–vapor phase change. The Pennes model has been employed as the most accepted bioheat model over a period of 60 years. Unlike other bioheat models which take account of arterial and venus temperature variations and the structure of local vasculature [30–34], the Pennes model treats the perfusion term as an isotropic heat sink. With the incorporation of the enthalpy method into the Pennes model, phase-change problems can be treated without the need of following the phase front as it moves through the tissue. To the best knowledge of the authors, the bioheat equation used here has not appeared in the published literature. The proposed bioheat equation is

$$\frac{\partial h_t}{\partial t} = k_t \frac{\partial^2 T_t}{\partial x^2} + (\rho c)_b \omega (T_{core} - T_t) + Q_{met} \tag{1}$$

The enthalpy per unit volume, thermal conductivity, density, and specific heat are represented by $h$, $k$, $\rho$, and $c$, respectively. The subscript t corresponds to the tissue which is regarded here as a composite of liquids, solids, and possibly water vapor. Subscript b is used for blood properties, and $\omega$ is the blood perfusion rate expressed as the volumetric flowrate per unit volume of tissue. $T_t$ and $T_{core}$ denote the local tissue and body core temperatures.

The physical process represented by the left-hand term in Eq. (1) is the change in the energy content of the tissue due both to temperature change and phase change. On the right-hand side, the first term accounts for heat conduction, which in the present application, is written in the one-dimensional form. The one-dimensional treatment is appropriate to the present situation because the convective heat transfer coefficients at the surface of the uterine lining are independent of location. Next, the second term on the right is the Pennes perfusion term. The other term, $Q_{met}$, is the metabolic heat generation rate.

To accommodate the phase change, the enthalpy must be given a three-part description. One part corresponds to temperature changes in the liquid-containing tissue, Eq. (2a); the second part accounts for the latent heat of evaporation, Eq. (2b); and the third part corresponds to the temperature changes in the post-phase-change tissue, Eq. (2c)

$$(\rho c)_t^{pre}(T_t - 37\,^\circ\mathrm{C}), \qquad 37 \leqslant T_t \leqslant 99\,^\circ\mathrm{C} \tag{2a}$$

$$h_t = \begin{cases} (\rho c)_t^{pre}(T_t - 37\,^\circ\mathrm{C}), & 37 \leqslant T_t \leqslant 99\,^\circ\mathrm{C} \\ h_t(99) + h_{fg} \cdot C_{liq} \cdot \frac{(T_t - 99\,^\circ\mathrm{C})}{(100 - 99\,^\circ\mathrm{C})}, & 99 < T_t \leqslant 100\,^\circ\mathrm{C} \end{cases} \tag{2b}$$

$$h_t(100) + (\rho c)_t^{post}(T_t - 100\,^\circ\mathrm{C}), \quad T_t > 100\,^\circ\mathrm{C} \tag{2c}$$

It can be seen from Eq. (2a) that the datum for the enthalpy has been set at 37 °C, without loss of generality. Between 37 °C and 99 °C, there is no phase change, and the enthalpy increases linearly with the temperature. The phase change is assumed to occur between 99 and 100 °C. The concentration of the liquid, $C_{liq}$, in the tissue is taken to be 79% [21]. The term $h_{fg}$ is the latent heat of evaporation. For temperatures in excess of 100 °C, it is assumed that no liquid is present, and the volumetric specific heat $(\rho c)^{post}$ is that of the solid portion of the tissue. The superscripts 'pre' and 'post' refer respectively to temperatures less than 99 °C and greater than 100 °C.

The dependence of the perfusion rate, $\omega$, on the state of the tissue is the least certain of all of the property specifications. The best available and most recently available information is for a porcine model [5]. Information from this paper was extracted to characterize the variation of perfusion throughout the heating process and was fitted by a polynomial which relates to the perfusion rate, $\omega$, to the Henriques–Moritz thermal damage integral, $\Omega$ [36]. The fitted equation is

$$\omega = \begin{cases} (1 + 25\Omega - 260\Omega^2)\omega_0, & 0 < \Omega \leqslant 0.1 \\ (1 - \Omega)\omega_0, & 0.1 < \Omega \leqslant 1 \end{cases} \tag{3}$$

The first of these equations reflects an initial increase in the perfusion rate as tissue is heated and vasodilation occurs. The second shows that as the heating process continues and cell injury accumulates, blood flow decreases as the vasculature begins to shut down (thrombosis). The term $\omega_0$ is the rate of perfusion in totally undamaged tissue [1,35].

The tissue injury integral is taken from [36] to be

$$\Omega(x,t) = \xi \int_0^t e^{-\left(\frac{\Delta E}{RT}\right)} d\lambda \tag{4}$$

Experimentally determined values of the $\xi$ and $\Delta E$ are available in the literature. For example, Baldwin et al. [1] reports the values of $\xi$ and $\Delta E$ as $3.1 \times 10^{98}\ s^{-1}$ and $6.27 \times 10^8$ J/kmole, respectively. The quantity $R$ is the universal gas constant whose value is 8.314 kJ/kmole K. The commonly accepted criterion for complete necrosis, $\Omega \cong 1$ [20], will be adopted here.

### 2.2. Physical properties

To complement the governing equations, Eqs. (1) and (2), it is necessary to provide values of the physical properties and other parameters that appear in Table 1.

It is relevant to contrast the present enthalpy-based bioheat equation, Eq. (1), with the approach used by Baldwin et al. [1], which is expressed by Eq. (13) of that paper. Careful examination of the latter equation leads to an uncertainty about whether it represents a field equation, valid throughout the tissue, or an interface equation which is applied at the boundary between the *pre* and *post* tissue.

Suppose first that Eq. (13) of [1] is considered to be an interface equation. A schematic diagram illustrating the physical situation is shown in Fig. 1. The figure shows a one-dimensional model which spans the tissue bed from

Table 1
Physical properties used in the numerical simulation

| Physical quantity | Value | Ref. | Physical quantity | Value | Ref. |
|---|---|---|---|---|---|
| $h_{fg}$ | $2.25 \times 10^6$ J/kg | | $T_{core}$ | 37 °C | |
| $(\rho c)_t^{pre}$ | $3.8 \times 10^6$ J/m$^3$ °C | [5,27] | $k_t^{pre}$ | 0.52 W/m °C | [25] |
| $(\rho c)_t^{post}$ | $4.4 \times 10^5$ J/10$^3$ °C | [5,27] | $k_t^{post}$ | 0.092 W/m °C | [25] |
| $(\rho c)_b$ | $4.1 \times 10^6$ J/m$^3$ °C | [5] | $\omega_0$ | 0.0028 s$^{-1}$ | [35] |

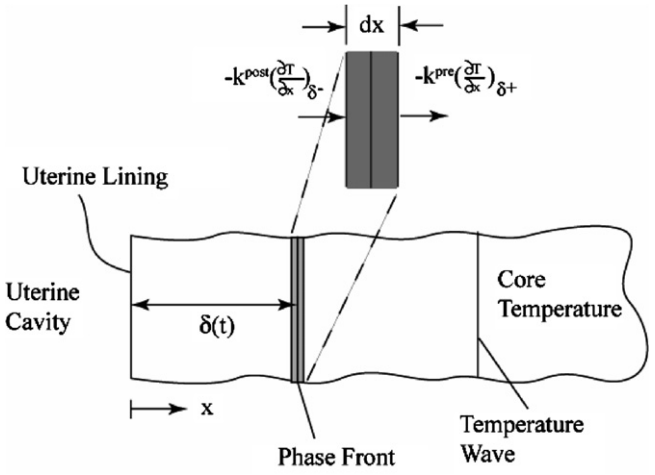


Fig. 1. Instantaneous locations of the phase front and temperature wave in a one-dimensional tissue model.

the uterine cavity at the left to the thermally undisturbed tissue at the right. The instantaneous location of the phase front, the liquid–vapor interface, is also shown. In addition, the temperature wave, created by the exposure of the uterine lining to the hot liquid in the uterine cavity, is indicated. The inset at the top of the diagram represents a control volume which spans the phase-change interface. The instantaneous energy inflows and outflows at the boundaries of the control volumes are called out in the inset. Due to the liquid–vapor phase change which occurs within the control volume, the energy inflow is necessarily greater than the energy outflow. The complete energy balance is

$$-k^{post}\left(\frac{\partial T}{\partial x}\right)_{\delta-} = -k^{pre}\left(\frac{\partial T}{\partial x}\right)_{\delta+} + h_{fg}\frac{d\delta}{dt} \tag{5}$$

In contrast to this energy balance, Baldwin et al. [1] uses an energy balance involving a second derivative $\partial^2 T/\partial x^2$. Since the derivatives $(\partial T/\partial x)_{\delta-}$ and $(\partial T/\partial x)_{\delta+}$ are discontinuous, it is mathematically impossible that their difference would yield a second derivative. In this light, it is believed that Baldwin et al.'s [1] Eq. (13) is not an energy balance at the phase-change interface.

The second possible interpretation of Baldwin et al.'s [1] Eq. (13) is that it is a field equation. However, the absence of a perfusion term in that equation argues against this interpretation. Furthermore, the presence of a phase-change term in Baldwin et al.'s equation (13) is inconsistent with the heat transfer processes which occur away from the phase-change front. These facts provide strong evidence against the interpretation of Baldwin et al.'s Eq. (13) as a field equation.

The preceding paragraphs cast some uncertainty about the model used by Baldwin et al. [1,3] for the investigation of phase change in tissue.

### 2.3. Initial and boundary conditions

The bioheat differential equation, Eq. (1), was solved by first discretizing it to obtain a set of algebraic equations. While the results presented here were obtained by using an explicit finite-difference solution method, others have utilized more complex numerical schemes for solving bioheat problems including Monte Carlo and variational calculus methods (for example, [37–40]). The spatial and temporal discretization was chosen to ensure solutions of sufficient accuracy. The initial conditions that were imposed on the solution are a uniform temperature of 37 °C throughout and a uniform liquid concentration of 79% [21]. Also required are boundary conditions at the two ends of the solution domain. At $x = 0$, the uterine lining, a temperature of 140 °C was imposed. The attainment of this temperature level can be achieved by the irrigation of the uterine cavity with a mixture of liquid water and an additive which increases the boiling point temperature; for instance, a 5% dextrose solution in water [1,3]. The use of water as the heating medium results in both high and spatially uniform heat transfer coefficients. The distal end of the solution domain was selected to be at $x = 15$ mm from the uterine lining. At that location, the temperature was assigned a value of 37 °C.

## 3. Results and discussion

### 3.1. Necrosis depths

Computations were performed for cases encompassing three levels of perfusion, with or without phase change, and constant properties versus variable properties. The results for the necrosis depths achieved during a 2-min and a 4-min therapeutic duration are presented in Figs. 2–4, respectively. Each of these figures is a bar graph whose heights indicate the depth of necrosis. Fig. 2 delineates the effect of variable properties; Fig. 3 is focused on the role of phase change; and Fig. 4 elucidates the influence of perfusion. In each figure, results are conveyed for two durations of the therapeutic period, 2 and 4 min, respectively.

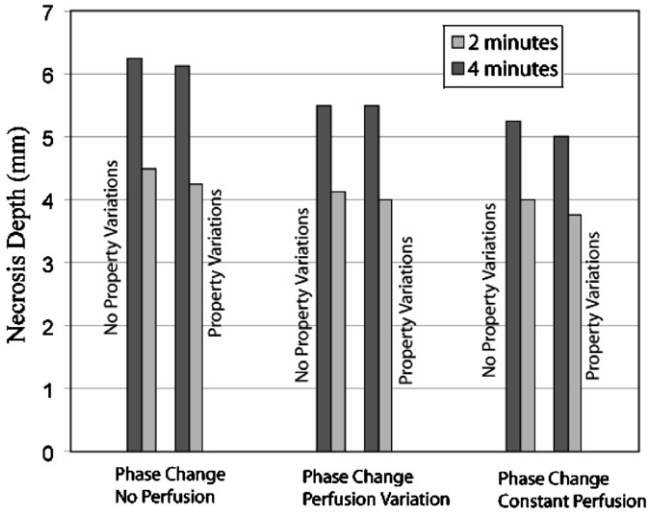


Fig. 2. Effect of property variations on necrosis depths for 2- and 4-min therapy durations.

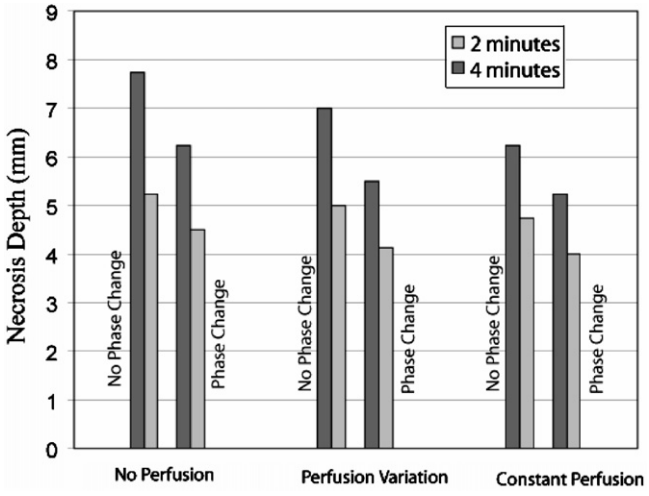


Fig. 3. Effect of phase change on necrosis depths for 2- and 4-min therapy durations.

Attention will first be directed to the results presented in Fig. 2. The results exhibited there are clustered into three groups, with each group being characterized by the extent of perfusion. All groups include phase change. Within each group, results are shown for the respective cases in which property variations are either accounted or omitted. In general, it can be seen that for all of the considered cases, the effect of property variations are minimal. Also noteworthy is the depth of necrosis achieved during the simulated therapy. For the 2-min duration, necrosis depths of approximately 4 mm are observed. When the therapy duration is increased to 4 min, necrosis depths of 5–6 mm are achieved.

The next figure, Fig. 3, focuses on the role of phase change. In this figure, the clusters of results are segregated according to the extent of the perfusion. Inspection of the figure reveals a major effect of phase change. When phase

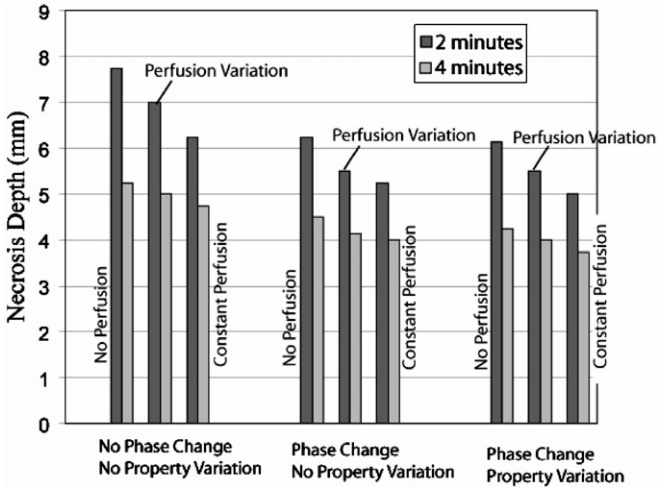


Fig. 4. Effect of perfusion variation on necrosis depths for 2- and 4-min therapy durations.

change is taken into account, necrosis depths are seen to decrease markedly. This behavior is due to the heat-sink nature of the phase-change process which intercepts the heat flow and prevents it from penetrating the tissue.

For instance, in the absence of perfusion, for the 4-min therapy duration, the respective necrosis depths without and with phase change are 7.75 mm and 6.25 mm.

The effects of various rates of perfusion are identified by the results conveyed in Fig. 4. As in Figs. 2 and 3, the results of Fig. 4 are clustered into three categories. The categories for Fig. 4 are the absence or presence of phase change and property variations. The three levels of perfusion indicated in the figure are: (a) the limiting case of no perfusion, (b) perfusion variations with necrosis according to Eq. (3), and (c) constant perfusion [35]. The figure shows that the rate of perfusion has a marked effect in altering the depth of necrosis. The no-perfusion cases show the greatest necrosis depths. The variable perfusion case exhibits lesser necrosis depths, and constant perfusion displays the least necrosis. This trend can be attributed to the fact that the variable perfusion model, Eq. (3), is based on a diminution of the constant perfusion rate, $\omega_0$. The decrease of necrotic depth with increasing perfusion can be explained by noting that the perfusive blood flow acts as a heat sink. In this regard, it is similar to the presence of phase change.

### 3.2. Criterion of necrosis

A detailed presentation of the method for the determination of the necrosis depth is set forth in Fig. 5. In the figure, the thermal injury integral, $\omega$, is plotted as a function of position in the tissue at the termination of a 4-min application of the therapy. The horizontal axis measures distances from the uterine lining. The figure contains six curves which are numbered according to Table 2. Each intersection between a $\omega$ curve and the line $\Omega = 1$ has been marked.

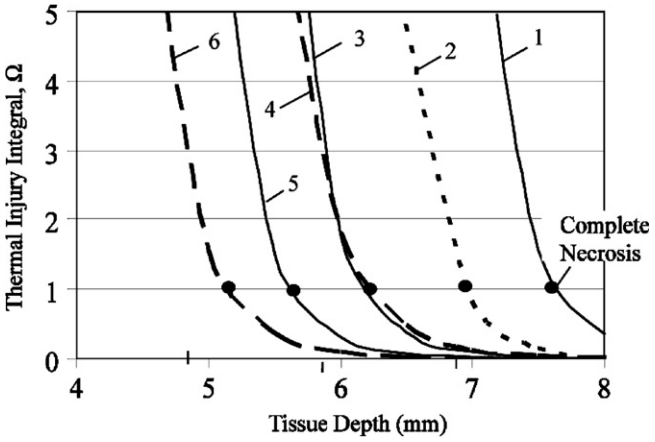


Fig. 5. Thermal injury achieved during a 4-min heating period. Necrosis was defined by the attainment of the value $\Omega = 1$ for the tissue injury integral, Eq. (4). Cases 1–6 are keyed to the descriptions in Table 2.

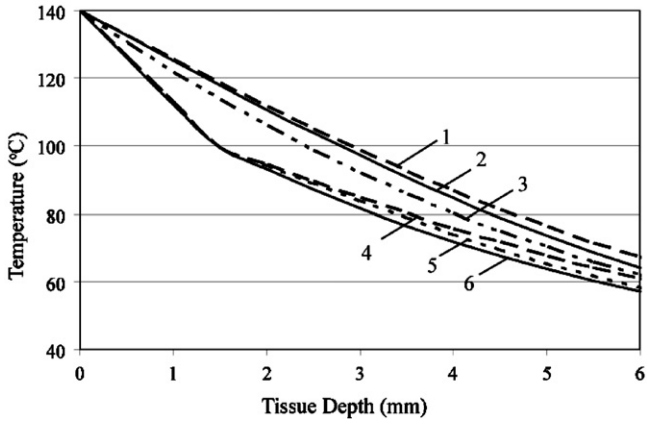


Fig. 6. Spatial temperature variations after a 2-min heating period for each of the investigated cases. Cases 1–6 are keyed to the descriptions in Table 2.

Table 2
Key to the results conveyed in Figs. 5–7

| Case no. | Phase change | Perfusion model |
|---|---|---|
| 1 | None | None |
| 2 | None | Variable |
| 3 | None | Constant |
| 4 | Yes | None |
| 5 | Yes | Variable |
| 6 | Yes | Constant |

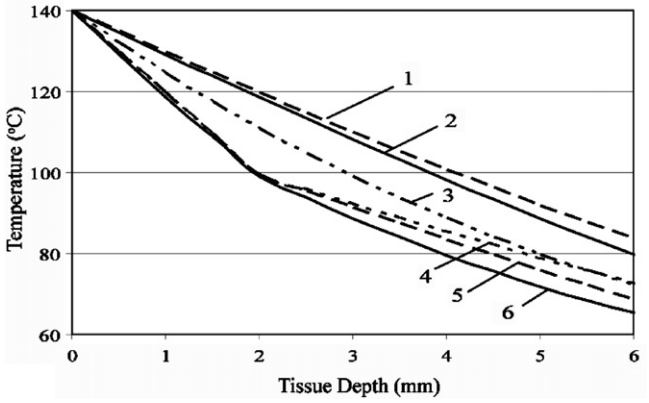


Fig. 7. Spatial temperature variations after a 4-min heating period for each of the investigated cases. Cases 1–6 are keyed to the descriptions in Table 2.

Inspection of the figure shows that the three cases without phase change (Cases 1–3) achieve notably deeper necrosis than do their counterparts which are characterized by phase change (Cases 4–6), respectively. This finding reinforces the information that was presented in Fig. 3.

### 3.3. Temperature distributions

The temperature distributions in the tissue at the termination of the 2- and 4-min heating durations are presented in Figs. 6 and 7, respectively. Each figure contains curves that are labeled according to Table 2. It can be seen from both of these figures that the cases which represent phase change (Cases 4–6) form a separate group from those without phase change (Cases 1–3). In particular, the phase-change cases are characterized by lower temperatures than those cases where there is no phase change. This behavior is consistent with the interpretation of the phase-change process as providing a sink of thermal energy at the liquid–vapor interface. These interfaces can be detected by the change of slope which is evident in the curves. The change of slope is demonstrated by Eq. (5). In contrast, the no-phase-change cases do not have a change of slope since the heat conduction is continuous.

These figures also enable the detection of the effects of constant perfusion versus variable perfusion. For example, Cases 1–3 differ among themselves only by the treatment of perfusion. In Case 1, the heat sink associated with perfusion drops out while in Cases 2 and 3, the heat sink remains. As a consequence, the temperatures for Cases 2 and 3 are lower than those for Case 1. A similar explanation can be offered for the spread among Cases 4 and 6.

## 4. Concluding remarks

A new bioheat equation, based on the enthalpy model of phase change, has been formulated and applied to the determination of the necrosis of tissue due to elevated temperatures. The thermophysical properties used in the model are explicit functions of the instantaneous, local moisture content of the tissue.

Numerical simulations have been carried out to predict necrosis depths encountered in endometrial ablation therapy for the treatment of menorrhagia. The key issues that were investigated were: (a) liquid-to-vapor phase change, (b) dependence of the properties of tissue on moisture

content, and (c) various perfusions models. The latter encompass the entire range of possible perfusion rates. One of these is the limit of no perfusion; a second is the case in which the rate of perfusion is a function of the degree of necrosis; and the third is a limit in which the perfusion is constant regardless of the status of the necrosis.

The results show that the accounting of phase change has a dominant effect on the depth of necrosis achieved as a result of the applied thermal therapy. In the presence of phase change, the necrosis depth decreases markedly. Perfusion was also found to have a major effect on necrosis depth, with higher rates of perfusion resulting in a lesser necrosis depth. The effect of moisture-dependent thermophysical properties was negligible.

The use of the enthalpy method eliminated the need to track the location of the phase-change front during the numerical calculations.

## Acknowledgements

Support of H. Birali Runesha and the Supercomputing Institute for Digital Simulation & Advanced Computation at the University of Minnesota is gratefully acknowledged.

## References

[1] S. Baldwin, A. Pelman, J. Bert, A heat transfer model of thermal balloon endometrial ablation, Ann. Biomed. Eng. 29 (2001) 1009–1018.
[2] B. Persson, B. Friberg, J. Olsrud, J. Rioseco, M. Ahlgren, Numerical calculations of temperature distributions resulting from intracavity heating of the uterus, Gyn. Endoscopy 7 (1998) 203–209.
[3] D. Reinders, S. Baldwin, J. Bert, Endometrial thermal balloon ablation using a high temperature, pulsed system: a mathematical model, J. Biomech. Eng. 125 (2003) 841–851.
[4] X. He, J. Bischof, Quantification of temperature and injury response in thermal therapy and cryosurgery, Crit. Rev. Biomed. Eng. 31 (2003) 355–421.
[5] X. He, S. Mcgee, J. Coads, F. Schmidlin, P. Iaizzo, D. Swanlund, S. Kluge, E. Rudie, J. Bischof, Investigation of the thermal and tissue injury behavior in microwave thermal therapy using a porcine kidney model, Int. J. Hyperthermia 20 (2004) 567–593.
[6] J. Liu, L. Zhu, L. Xu, Studies on the three-dimensional temperature transients in the canine prostate during transurethral microwave thermal therapy, J. Biomech. Eng. 122 (2000) 372–379.
[7] L. Xu, E. Rudie, K. Holmes, Transurethral thermal therapy (T3) for the treatment of benign prostate hyperplasia (BPH) in the canine: analysis using Pennes bioheat equation, HTD 268, in: Advances in Bioheat and Mass Transfer: Microscale Analysis of Thermal Injury Processes, Instrumentation, Modeling, and Clinical Applications, American Society of Mechanical Engineers, New York, 1993.
[8] L. Xu, L. Zhu, K. Holmes, Blood perfusion measurements in the canine prostate during transurethral hyperthermia, Ann. New York Acad. Sci. 858 (1998) 21–29.
[9] D. Yuan, J. Valvano, E. Rudie, L. Xu, 2D finite difference modeling of microwave heating in the prostate, HTD 322/BED 32, in: Advances in Heat and Mass Transfer in Biotechnology, American Society of Mechanical Engineers, New York, 1995.
[10] J. Zhang, G. Sandison, J. Murthy, L. Xu, Numerical simulation for heat transfer in prostate cancer cryosurgery, J. Biomech. Eng. 127 (2005) 279–293.
[11] J. Zhou, J. Liu, Numerical study on 3d light and heat transfer in biological tissue with large blood vessels during laser-induced thermotherapy, Numer. Heat Transfer A 45 (2004) 415–449.
[12] N. Shamsundar, E. Sparrow, Analysis of multidimensional conduction phase change via the enthalpy method, J. Heat Transfer 97 (1975) 333–340.
[13] V. Voller, Numerical methods for phase change problems, in: W.J. Minkowycz, E.M. Sparrow, J.Y. Murthy (Eds.), Handbook of Numerical Heat Transfer, second ed., John Wiley and Sons, Hoboken, 2006.
[14] V. Voller, M. Cross, Accurate solutions of moving boundary problems using the enthalpy method, Int. J. Heat Mass Transfer 24 (1981) 545–556.
[15] G. Bell, On the performance of the enthalpy method, Int. J. Heat Mass Transfer 25 (1982) 587–589.
[16] K. Udell, The thermodynamics of evaporation and condensation in a porous media heated from above with evaporation, condensation, and capillary effects, J. Heat Transfer 105 (1983) 482–492.
[17] K. Udell, Heat transfer in porous media considering phase change and capillarity – the heat pipe effect, Int. J. Heat Mass Transfer 28 (1985) 485–495.
[18] Q. Pham, A fast unconditionally stable finite-difference scheme for heat conduction with phase change, Int. J. Heat Mass Transfer 28 (1985) 2079–2084.
[19] N. Bhavaraju, J. Valvano, Thermophysical properties of swine myocardium, Int. J. Thermophys. 20 (1999) 665–676.
[20] K. Diller, J. Valvano, J. Pearce, Bioheat transfer, in: F. Kreith (Ed.), CRC Handbook of Thermal Engineering, CRC Press, Boca Raton, 2000.
[21] F. Duck, Physical Properties of Tissue, Academic Press, London, 1990, pp. 9–42.
[22] J. Olsrud, B. Friberg, M. Ahlgren, B. Persson, Thermal conductivity of uterine tissue in vitro, Phys. Med. Biol. 43 (1998) 2397–2406.
[23] T. Cooper, G. Trezck, Correlation of thermal properties of some human tissues with water content, Aerosp. Med. 42 (1971) 24–27.
[24] R. Skalak, R. Chien, Handbook of Bioengineering, McGraw-Hill, New York, 1987.
[25] K. Spells, The thermal conductivities of some biological fluids, Phys. Med. Biol. 5 (1960) 139–152.
[26] A. Takata, L. Zaneveld, W. Richter, Laser-induced thermal damage in skin. USAF School Aerospace Med. Brooks AFB, TX, Rep. SAM-TR-77-38, 1977.
[27] A. Welch, The thermal response of laser irradiated tissue, J. Quant. Electron. 20 (1984) 1471–1481.
[28] L. Hayes, K. Diller, A finite element model for phase change heat transfer in a composite tissue with blood perfusion, ISA Trans. 22 (1983) 33–37.
[29] H. Pennes, Analysis of tissue and arterial blood temperatures in the resting human forearm, J. Appl. Physiol. 85 (1948) 5–34.
[30] Y. Xuan, W. Roetzel, Transient response of the human limb to an external stimulus, Int. J. Heat Mass Transfer 41 (1998) 229–239.
[31] S. Weinbaum, L. Jiji, A two-phase theory for the influence of circulation on heat transfer in surface tissue, ASME, New York 79-WA/HT-72, 1979.
[32] S. Weinbaum, L. Jiji, D. Lemons, Theory and experiment for the effect of vascular microstructure on surface tissue heat transfer – part I: anatomical foundation of model conceptualization, J. Biomech. Eng. 106 (1984) 321–330.
[33] E. Wissler, Comments on the new bioheat equation proposed by Weinbaum and Jiji, J. Biomech. Eng. 109 (1987) 226–233.
[34] Y. He, H. Liu, R. Himeno, A one-dimensional thermo-fluid model of blood circulation in the human upper limb, Int. J. Heat Mass Transfer 47 (2004) 2735–2745.
[35] R. Wynn, Biology of the Uterus, Plenum, New York, 1977.
[36] F. Henriques, A. Moritz, Studies of thermal injury I: the conduction of heat to and through the skin and the temperatures attained therein. A theoretical and experimental investigation, Am. J. Pathol. 23 (1947) 531–549.

[37] W. Dai, H. Yu, R. Nassar, A fourth-order compact finite difference scheme for solving a 1-d Pennes bioheat transfer equation in a triple-layered skin structure, Numer. Heat Transfer B 46 (2004) 447–461.
[38] Z. Deng, J. Liu, Monte Carlo method to solve multidimensional bioheat transfer problems, Numer. Heat Transfer B 42 (2002) 543–567.
[39] T. Loulou, E. Scott, Thermal dose optimization in hyperthermia treatments by using the conjugate gradient method, Numer. Heat Transfer A 42 (2002) 661–683.
[40] W. Dai, R. Nassar, A numerical method for optimizing laser power in the irradiation of a 3D triple-layered skin structure, Numer. Heat Transfer A 48 (2005) 21–41.